



DEFENCE RESEARCH ESTABLISHMENT
CENTRE DE RECHERCHES POUR LA DÉFENSE
VALCARTIER, QUÉBEC



DREV TM-2000-007

Unlimited Distribution / Distribution illimitée

A NUMERICAL ANALYSIS OF THE EFFECT
OF SURROGATE ANTI-TANK MINE BLASTS ON THE M113

by

K. Williams

K. Poon*

March/mars 2000

*Research Assistant,
University of British Columbia

RESEARCH AND DEVELOPMENT BRANCH
DEPARTMENT OF NATIONAL DEFENCE
CANADA
BUREAU - RECHERCHE ET DÉVELOPPEMENT
MINISTÈRE DE LA DÉFENSE NATIONALE

DTIC QUALITY INSPECTED 3

20000404 004

UNCLASSIFIED

DEFENCE RESEARCH ESTABLISHMENT
CENTRE DE RECHERCHES POUR LA DÉFENCE
VALCARTIER, QUEBEC

DREV TM-2000-007

Unlimited Distribution / Distribution illimitée

A NUMERICAL ANALYSIS OF THE EFFECT
OF SURROGATE ANTI-TANK MINE BLASTS ON THE M113

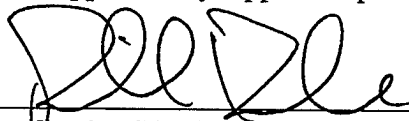
by

K. Williams
K. Poon*

March/mars 2000

*Research Assistant,
University of British Columbia

Approved by /approuvé par



Section Head/Chef de section

Date

SANS CLASSIFICATION

WARNING NOTICE

The information contained herein is proprietary to Her Majesty and is provided to the recipient on the understanding that it will be used for information and evaluation purposes only. Any commercial use, including use for manufacture, is prohibited. Release to third parties of this publication or of information contained herein is prohibited without the prior written consent of DND Canada.

© Her Majesty the Queen in Right of Canada as represented by the Minister of National Defence, 2000

ABSTRACT

This memorandum summarises numerical analyses which were performed to investigate the use of a simple empirical impulse loading model as a tool for modelling blast mine loading on a structure. The empirical model was used to generate the initial velocity boundary condition for an explicit dynamic finite element analysis of the floor deformation of a simulated M113 MTVL (upgraded floor protection) subject to the detonation of a buried 7.5-kg C-4 mine surrogate. Results showed an over-prediction of the peak residual floor deflection. Reducing the impulse by 33% gave excellent agreement with experimental results. The need to scale the impulse is attributed to energy absorption in the soil through mechanisms that are not accounted for in the empirical model. Moisture content and soil type, for example, are known to significantly affect the apparent strength of blast mines.

RÉSUMÉ

Ce mémorandum résume les analyses numériques de l'utilisation d'un modèle empirique d'impulsion comme outil de modélisation du chargement d'une structure provoqué par le souffle d'une mine. Le modèle empirique a été utilisé pour dériver les contraintes de vitesse initiale pour une analyse dynamique par éléments finis explicites de la déformation du plancher d'un M113 MTVL simulé (protection améliorée du plancher) provoquée par la détonation d'une mine antichar sous le ventre du véhicule. Les résultats ont démontré une surestimation du déplacement résiduel du plancher. Une diminution de l'impulsion de 33% a donné des résultats qui concordent avec les résultats expérimentaux. La raison pour laquelle l'impulsion doit être diminuée est probablement liée à des mécanismes d'absorption d'énergie dans le sol dont on ne tient pas compte dans le modèle empirique. Par exemple, le contenu de l'eau et le type de sol sont reconnus comme des quantités qui ont un effet significatif sur la puissance de poussée de la mine.

TABLE OF CONTENTS

ABSTRACT	I
EXECUTIVE SUMMARY	IV
LIST OF SYMBOLS.....	VI
1.0 INTRODUCTION.....	1
2.0 MODEL DESCRIPTION.....	3
2.1 FINITE ELEMENT MESH	3
2.2 MATERIAL MODELS	6
2.3 BOUNDARY CONDITIONS.....	6
2.4 SPRINGBACK CALCULATION.....	9
3.0 COMPUTATIONAL RESULTS AND DISCUSSION	10
3.1 FULL IMPULSE SIMULATION	10
3.2 SCALED IMPULSE SIMULATIONS	11
3.3 PREDICTED FLOOR DEFORMATION	12
3.4 IMPLICATIONS OF SCALING THE IMPULSE	16
4.0 CONCLUSION	18
5.0 ACKNOWLEDGEMENTS	19
6.0 REFERENCES	20
FIGURES 1 to 13	
TABLES I to III	

EXECUTIVE SUMMARY

In recent years, Canadian Forces on UN peacekeeping missions have suffered a number of casualties as a direct result of landmines. A majority of landmine accidents have involved vehicles. The development of mine protection systems to decrease the vulnerability of vehicles and, more importantly, of their crews requires an accurate assessment of the effects of the blast on the vehicle structure and armour. To better understand these effects, the Defence Research Establishment Valcartier has undertaken a research and development program that focuses on numerical modelling of light armoured and soft-skinned vehicles subjected to detonations of blast mines.

Modelling mine blast effects on vehicles can be divided into two tasks. One is modelling the structural response of the vehicle. The other involves modelling the detonation of the mine and the transmission of the energy of the blast to the vehicle through pressure wave propagation through the soil and air and through momentum transfer from the blast ejecta (soil and detonation products). While current hydrocodes are capable of modelling large strain, high rate deformation for most materials, detailed detonation and blast modelling for mines is less advanced. Work in this area is currently being funded jointly by the Defence Research Establishments Valcartier and Suffield but the modelling techniques will require another year or more of development before they can be applied to practical problems. As an interim solution, an empirical loading model is being investigated as a tool to generate the boundary conditions for a finite element analysis of the structural response of a vehicle. Experimental results for floor deflection of a modified M113A2 vehicle, with upgraded floor protection to simulate the MTVL variant, were used to validate this approach. A finite element model of the vehicle was assembled and subjected to the impulse loading generated by the empirical model for a 7.5-kg C-4 mine surrogate, the charge used in the experimental trial.

Initial results indicated that the predicted floor deflection was much greater than that measured experimentally. This over prediction of the impulse generated by the mine is attributed to the inability of the empirical mine impulse model to account for variations in the soil type, moisture content, and other soil properties which are known to

UNCLASSIFIED

v

significantly influence the effective blast strength of a buried mine. The experimental results were used to calibrate the impulse. Reducing the impulse by 33% resulted in floor deflections that matched the measured residual deflections.

The next stage in the project is to apply the calibrated impulse loading model to the other test configurations that made up the test matrix on the modified and unmodified M113A2 and to other target geometries. This work will further validate the use of the calibrated empirical model as a tool for predicting the effects of blast mines on structures.

LIST OF SYMBOLS

A_{mine}	planar cross-sectional area of the mine (m^2)
A_{plate}	presented area of the plate (m^2)
d	depth of burial of the mine (m)
D_{mine}	diameter of the mine (m)
E	elastic modulus (MPa)
E_T	tangent modulus (MPa)
$\{i\}$	impulse vector (Pa s)
i_z	vertical component of the specific impulse (Pa s)
m_{mine}	mass of the mine (kg)
m_{plate}	plate mass (kg)
r	distance from the geometric centre of the mine (m)
s	stand-off distance of the plate from the mine (m)
v_n	initial velocity (m/s)
W	energy release of the mine (J)
n_{TNT}	explosive TNT equivalency factor
ϵ_f	failure strain
ν	Poisson's ratio
ρ	density, (kg/m^3)
ρ_{plate}	plate density (kg/m^3)
ρ_{soil}	density of the soil (kg/m^3)
σ_Y	yield stress (MPa)

1.0 INTRODUCTION

Design of improved anti-mine protection systems traditionally requires extensive experimental test programs to validate their effectiveness in reducing the vulnerability of the vehicle and the vehicle occupants to blast mines (see Fig. 1). These test programs are extremely time consuming and expensive and they usually involve destructive testing of the vehicle. Not only does this add significantly to the cost of development but it generally restricts the type of truck or armoured personnel carrier (APC) that can be tested to vehicles that are either damaged beyond repair (rare) or being phased out of service. Evaluation of newly or soon to be acquired vehicles is generally out of the question. By developing and verifying numerical tools to analyse the effects of mine blast on vehicles, it is possible to predict, to an acceptable degree of accuracy, the vulnerability of those vehicles to blast loading.



FIGURE 1 – Example of the floor deformation resulting from the detonation of a 7.5-kg C4 surrogate mine under an unprotected M113 APC. In the photograph, the vehicle is shown lying on its side. At the top left corner is one of the road wheels.

DREV is conducting a broad program on numerical simulation of mine blast events. One of the aims of this research is vehicle vulnerability. This work can be divided into two tasks: accurately modelling the vehicle response and accurately modelling the mine blast and its effects on the vehicle. This memorandum describes one of the projects that is focusing on the latter, the mine blast effects. The primary objective of this work is to validate the use of a simple representation of the mine blast, through an impulse boundary condition, as a numerical tool for predicting the floor deformation of a light armoured vehicle which has detonated an anti-tank blast mine.

The development of numerical models for predicting the detailed pressure loading and momentum transfer histories that result from the detonation of a blast mine is being funded by the Defence Research Establishments Valcartier and Suffield (DREV and DRES). The development work is focused on a combined computational fluid dynamics (CFD) and computational structural dynamics (CSD) approach. However, it appears that it will be a year or more before these numerical models are at a stage where they can be applied to practical problems. As a result, an analytical model by Westine *et al.* (Ref. 1) has been used to predict the loading on the vehicle by the blast debris and detonation products of a blast mine. This analytical model is based on an empirical equation fit to experimental data and is adapted, using work by Morris (Ref. 2) and Tremblay (Ref. 3), to predict the initial velocity distribution of the floor of a vehicle.

Validation of the numerical study described here is based on experimental results. During the experimental program described by St-Jean (Ref. 4), a series of tests were conducted in which 7.5-kg (126.5-lb) C-4 mine surrogates (buried cylindrical charges of C-4 used to simulate a blast mine) were detonated under the track and under the hull of scrap M113 tracked APCs. Two vehicle configurations were studied; the baseline bare M113A2 and an M113A2 modified to simulate the Mobile Tactical Vehicle Light (MTVL) configuration. The MTVL vehicle has a 19-mm (0.75-in) steel plate augmenting the floor protection. An under hull detonation on the MTVL configuration was selected as the basis for the numerical study described in this memorandum. Unfortunately, no tests were performed for under hull detonations on the bare M113A2 and the tests involving charges buried under the tracks were not simulated here because

of the added complexity involved in modelling the interaction between the track, wheels, and suspension and the blast. This task is left for future work when numerical techniques available for modelling blast mine effects will be more advanced.

This work was performed at the DREV between July and November 1999 under Work Unit 2fg16, "LAV Mine Protection Technical Demonstrator".

2.0 MODEL DESCRIPTION.

The hydrodynamic explicit finite element (FEM) code LS-DYNA3D (Ref. 5) was used to perform the numerical analyses. The LS-DYNA family of codes have been used extensively by government research laboratories and industry for analysing the large deformation and high strain rate response of inelastic structures.

2.1 Finite Element Mesh

A solid model of the M113A2 was built using the FEMAP 6.0 CAE package (Ref. 6). The completed model includes all major structural elements of the vehicle except the engine, which will be added shortly. A three dimensional hexagonal element meshed version of the solid model is shown in Fig. 2.

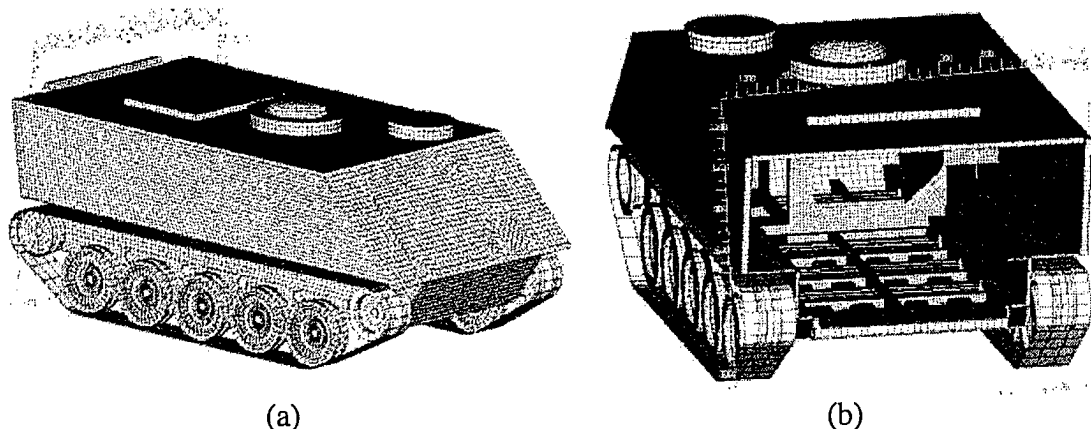


FIGURE 2 – Full M113A2 solid model meshed using brick elements showing (a) the tracks, wheel, suspension, and (b) the internal structure (the rear wall and ramp have been removed)

It is important to highlight that the goal of the analyses was to predict the floor deflection and not the overall rigid body dynamics of the vehicle. Experimental evidence, in the form of high-speed video, indicates that the floor deflection occurs before there is significant rigid body motion of the vehicle (Ref. 4). It is therefore reasonable to assume that the added inertia from the doors, hatches, and other structures plays a minor role in the floor deflection. This is also true of the engine if the blast occurs away from the position of the engine, as is the case in this study. However, the engine could provide a stiffening effect to the floor structure for a blast under the front of the vehicle. Other structures ignored in the analyses were the tracks, wheels, and suspension. While the wheels and, to a lesser extent the tracks, influence the blast effect by reducing venting of the detonation products, this was assumed to have a secondary effect on the floor deflection. Venting and the suspension system response would be more important if the overall dynamics of the vehicle (e.g. rigid body motion) were being modelled.

Based on these assumptions, a simplified version of the M113A2 model was created for the current study. A shell model of the M113 hull was built using the midsurface of the walls of the vehicle as a reference surface. The FEM mesh, shown in Fig. 3, contains 10 270 quadrilateral elements and 10 301 nodes. The computationally efficient, Belytschko-Lin-Tsay co-rotational quadrilateral shell element is used throughout the model. The FEM model is divided into 9 parts, each of which defines a different plate section property (i.e. different material and/or thickness). This includes the RHA steel plate which is also modelled using quadrilateral shell elements (an additional 1120 elements and 1189 nodes). The steel plate is spaced 20 mm from the aluminum hull of the M113 and covers the rear two thirds of the floor. On the test vehicles, the plate was attached using bolts around the periphery of the plate. These bolts sheared off during the experimental tests and they were not considered in the numerical model. As a result, the steel plate is assumed to be free floating under the floor.

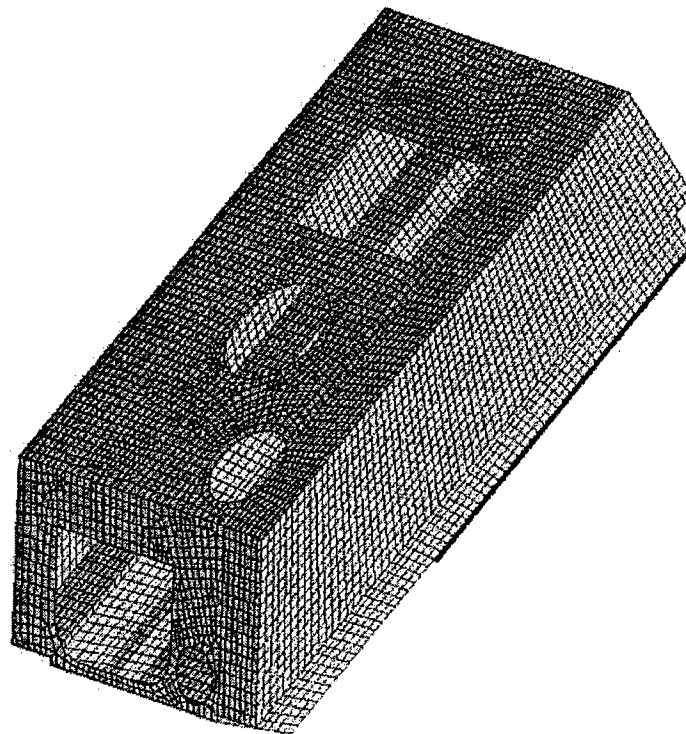
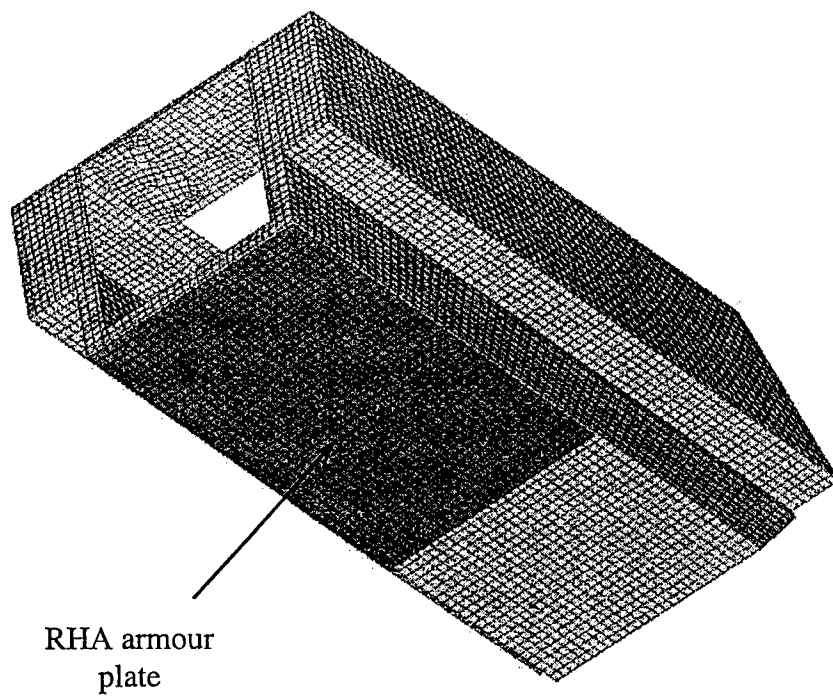


FIGURE 3 – Finite element mesh of the M113 shell model including the add-on RHA armour steel plate

2.2 Material Models

A kinematic/isotropic elastic-plastic hydrodynamic constitutive model was used for the aluminum hull and steel armour. The model predicts a bilinear stress-strain behaviour. Strain rate effects were not considered for this preliminary analysis. Material properties used for the M113 hull and armour plate are shown in Table I. Material failure was not considered in the analysis as rupture of the hull played a minor role in the overall deformation of the floor observed experimentally. However, material failure, in particular weld line failure, will be investigated in follow on work.

TABLE I
Material properties used for the M113 hull and armour plate

Property	M113 Hull	Armour Plate	Units
Material	Al 5086 H32	Steel	-
Density, ρ	2768	7850	kg/m ³
Elastic Modulus, E	73 080	197 500	MPa
Poisson's Ratio, ν	0.34	0.33	-
Yield Stress, σ_Y	335	900	MPa
Tangent Modulus, E_T	664	1810	MPa

2.3 Boundary Conditions

The impulse of the detonation products was assumed to act only on the steel plate which subsequently impacts the floor of the vehicle. The empirical equations developed by Westine *et al.* (Ref. 1) were used to calculate an initial nodal velocity which was applied to the nodes in steel plate.

2.3.1 Initial Velocity Model

The model by Westine *et al.* (Ref. 1) is derived from an experimental fit and gives a relationship between the specific impulse, i_z (Pa s), imparted on a horizontal plate as a function of the distance, r (m), from the geometric centre of the mine:

$$i_z = 0.1352 \left(\frac{\tanh(0.9589 P_S)}{P_S} \right)^{3.25} \frac{\rho_{soil}^{1/2} W^{1/2} \left(1 + \frac{7d}{9s} \right)}{s^{1/2}} \quad (1)$$

where

$$P_S = \frac{r d}{s^{5/4} A_{mine}^{3/8} \tanh \left(2.2 \frac{d}{s} \right)^{3/2}} \quad (2)$$

and d (m) is the depth of burial of the mine, s (m) is the stand-off distance of the plate from the mine, $A_{mine} = \pi D_{mine}^2 / 4$ (m^2) is the planar cross-sectional area of the mine, W (J) is energy release of the mine, and ρ_{soil} (kg/m^3) is the density of the soil (see Fig. 4). The energy release of the mine, W , is calculated from the energy content of TNT (4.516 MJ/kg), the mass of explosive, m_{mine} (kg), and the TNT equivalency factor, n_{TNT} (e.g. $n_{TNT} = 1.127$ for C-4):

$$W = n_{TNT} \cdot m_{mine} \cdot 4.516 \text{ MJ / kg} \quad (3)$$

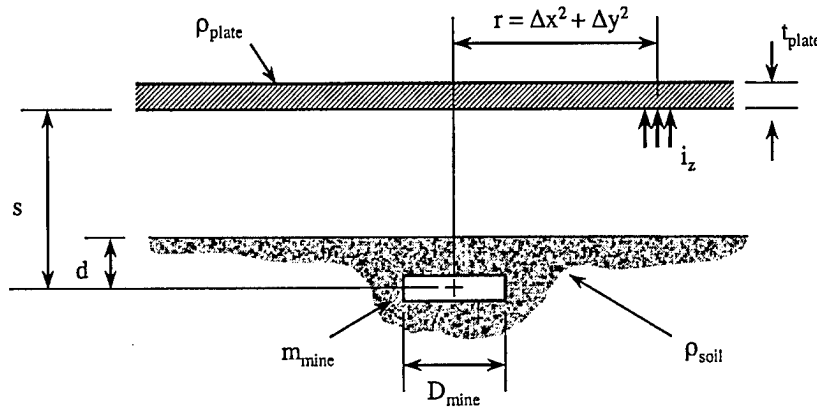


FIGURE 4 - Nomenclature used in the analytical specific impulse equation (adapted from Morris (Ref. 2))

From the normal impulse we can calculate the initial velocity, v_n (m/s), of an incremental unit of the plate with presented area A_{plate} (m^2), mass m_{plate} (kg), and thickness t_{plate} (m):

$$v_n = \frac{I}{\Delta m_{plate}} = \frac{(i_z \cdot A_{plate})}{m_{plate}} \cdot \frac{t_{plate}}{t_{plate}} = \frac{i_z}{\rho_{plate} \cdot t_{plate}} \quad (4)$$

where ρ_{plate} (kg/m³) is the plate density.

Therefore, in an FEM description of a problem, given the density of the soil, the description of the mine (W , d , and D_{mine}) and its location, the thickness and density of the plate, and the co-ordinate of the nodes on the plate, one can calculate the initial nodal velocity distribution. The equations presented above have been implemented as a Microsoft Windows® application which uses the LS-DYNA3D input deck written by FEMAP 6.0 to generate the initial nodal velocity for the LS-DYNA3D input deck based on the nodal co-ordinates, element normals, plate properties, and mine and soil properties.

The properties of the mine used in this study are shown below in Table II.

TABLE II
C-4 charge and soil properties

Parameter	Value
d	0.13 m
s	0.51 m
D_{mine}	0.203 m
m_{mine}	7.5 kg
n_{TNT}	1.129
W	38.23 MJ
ρ_{soil}	2170 kg/m ³

The location of the mine used for this particular test is shown in Fig. 5. The distance between the surface of the soil and the bottom of the armour plate is 0.38 m.

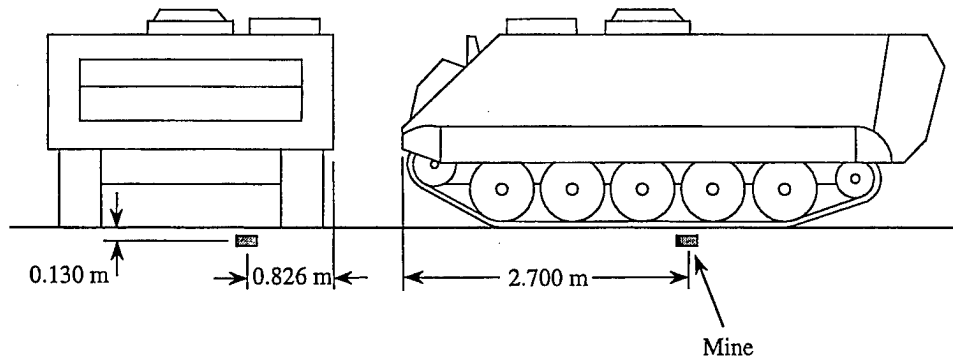


FIGURE 5 - Location of the surrogate mine

The initial velocity boundary conditions were only applied to the nodes of the steel plate. Although the plate does not shield the forward part of the floor of the M113, the impulse imparted to this region, which is remote from the mine, is very small in comparison to the impulse on the plate over the mine. No other displacement constraints were applied and the vehicle was free to move. As mentioned previously, experimental observations indicated that the floor deformation occurred before any significant rigid body motion. The acceleration due to gravity was not considered.

2.3.2 Validity of the Initial Velocity Model

The argument used to support the use of an initial velocity derived from a specific impulse equation is based on the duration of the loading. Morris (Ref. 2) argues that the natural period of the structural elements of a vehicle is much shorter than the duration of the loading (a few milliseconds) which results from the impact of the blast products and soil ejecta on the structure. As a result, a detailed knowledge of the pressure history is not required. Instead, the integral of the pressure time history (i.e. the impulse) is sufficient to represent the structural loading.

2.4 Springback Calculation

The highly dynamic nature of the blast loading results in an elastic oscillation of the deformation. These elastic waves are damped out after a few tenths of a second. While LS-DYNA excels at solving problems involving large strains and high rate deformation, it is not the most efficient tool to use for events that have a duration on the order of a second or more, particularly if they are dominated by elastic strains. Instead a

so-called springback calculation can be used to predict the residual deformation of the hull. Springback analyses are typically associated with metal forming operations where the final shape of a part is desired after it has been removed from the tooling. A springback analysis is generally performed using an implicit FEA code. All boundary conditions used in the explicit dynamic analysis are removed and replaced by the minimum number of displacement constraints required to eliminate rigid body motion. A multi-step implicit calculation is then used to calculate the residual stresses and deformation based on the elastic and plastic stresses in the system at the end of the explicit calculation.

A non-linear springback analysis for the M113 simulations was performed using a feature of LS-DYNA3D that automatically generates an LS-NIKE3D input deck and stress initialisation file at the end of a run. LS-NIKE3D (Ref. 7) is an implicit solver distributed with LS-DYNA3D by the Livermore Software Technology Corporation (note: the latest version of LS-DYNA, version 950, has a built-in implicit solver allowing a completely integrated solution). The LS-NIKE3D input deck generated by LS-DYNA3D was modified based on suggestions made in the LSTC "User's Guide to Coupled Springback Calculations using LS-DYNA3D and LS-NIKE3D" (Ref. 8). These modifications include changes to the artificial stabilisation and time step control.

3.0 COMPUTATIONAL RESULTS AND DISCUSSION

3.1 Full Impulse Simulation

The base line analysis used the full impulse predicted by Eqn. 1. The peak initial velocity was 365 m/s and the model was run for a total of 200 ms after which a springback analysis was performed. Fig. 6 shows the predicted peak floor deflection history along with the predicted residual floor deflection from the LS-NIKE3D springback analysis discussed in Section 2.4. Note that the residual deformation predicted by LS-NIKE3D falls right in the middle of the elastic oscillation from the LS-DYNA3D simulation, as one would expect. The residual deformation predicted is 578 mm, twice the experimental measurement of 287 mm made by St-Jean (Ref. 4).

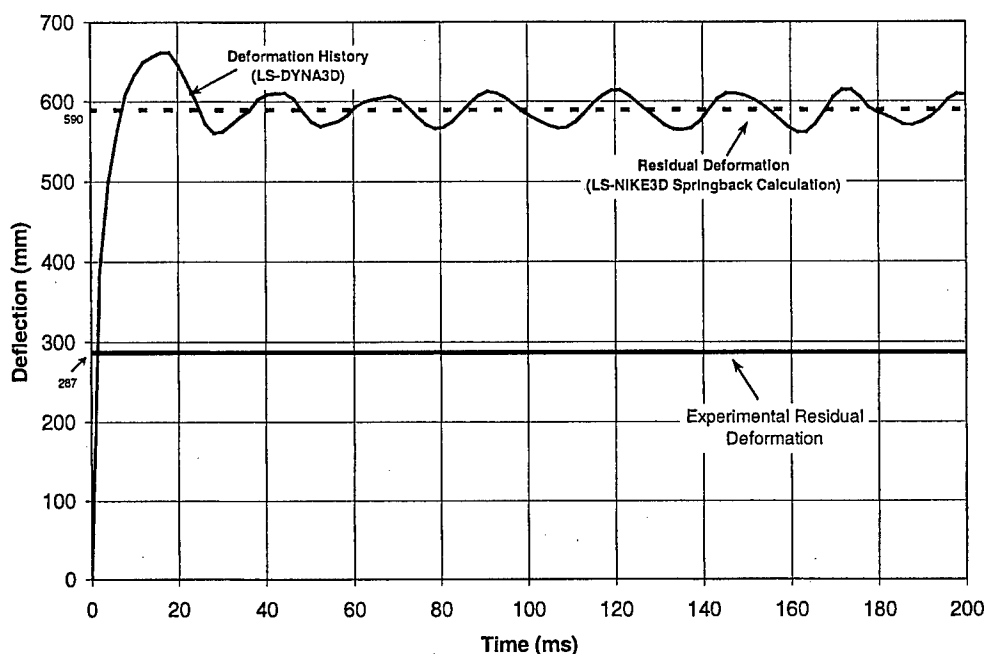


FIGURE 6 - Predicted peak floor deformation history for a 7.5-kg (16.5-lb) C-4 charge

A number of factors can explain the large difference between the predicted and measured values. The good agreement found by Morris (Ref. 2) seems to indicate that the mathematical model for the impulse is accurate. However it is well known that the effectiveness of a blast mine is extremely sensitive to the soil conditions including temperature, moisture content, and type of soil (e.g. sand or clay). Higher water content, for example, results in a stiffer, more incompressible soil which directs more of the explosive energy upwards. Lower soil density absorbs more the energy of the blast resulting in less damage to structures over the detonation. The empirical model accounts for all these effects through a single variable, the soil density, and it is likely that the soil conditions at the site used to derive the empirical relation are quite different from those at the DREV test range.

3.2 Scaled Impulse Simulations

Lacking guidance on how to modify the empirical equations, a simple approach was used to calibrate the analytical impulse model. A series of simulations were performed with initial velocities based on 33%, 50%, and 75% of the full impulse

predicted by Eq. 1. The peak initial velocities predicted by scaling the impulse are summarised in Table III below. The dependence of the predicted residual peak deformation on the impulse applied is shown in Fig. 7. The impulse scaling factor required to fit the experimental results is estimated from Fig. 7 to be 66%.

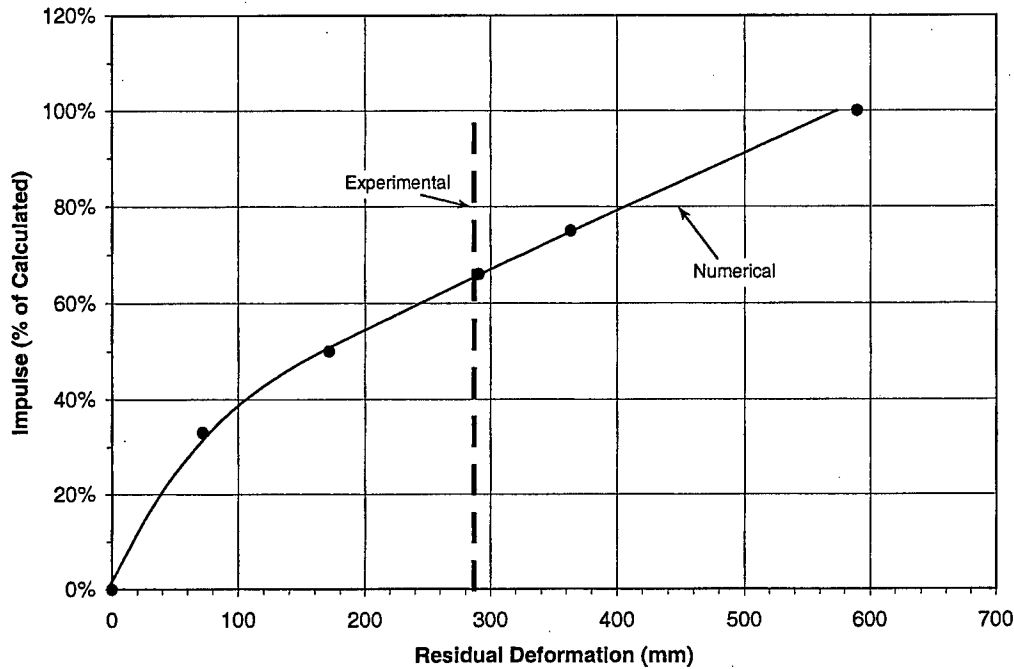


FIGURE 7 - Relationship between the peak residual deformation and the applied impulse as a percentage of the full impulse predicted by the empirical equations from Westine *et al.* (Ref. 1)

3.3 Predicted Floor Deformation

The results of the analysis with a 66% scaled impulse give a residual deformation of 291 mm, extremely close to the experimental result of 287 mm. Table III summarises the peak initial velocity and the predicted peak and residual deformation corresponding to each of the impulse scaling factors used. Fig. 8 summarises the deformation histories for all the simulations.

TABLE III
Initial velocity, effective charge size and deformation results

Impulse Scaling Factor	Peak Initial Velocity	Effective Charge	Peak Deformation		
			Maximum	Residual*	Elastic
100%	365 m/s	7.50 kg	661 mm	590 mm	71 mm
75%	274 m/s	4.22 kg	437 mm	364 mm	73 mm
66%	241 m/s	3.27 kg	353 mm	291 mm	63 mm
50%	182 m/s	1.87 kg	223 mm	172 mm	52 mm
33%	120 m/s	0.82 kg	114 mm	72 mm	41 mm

* The experimentally measured residual deformation is 287 mm (Ref. 4).

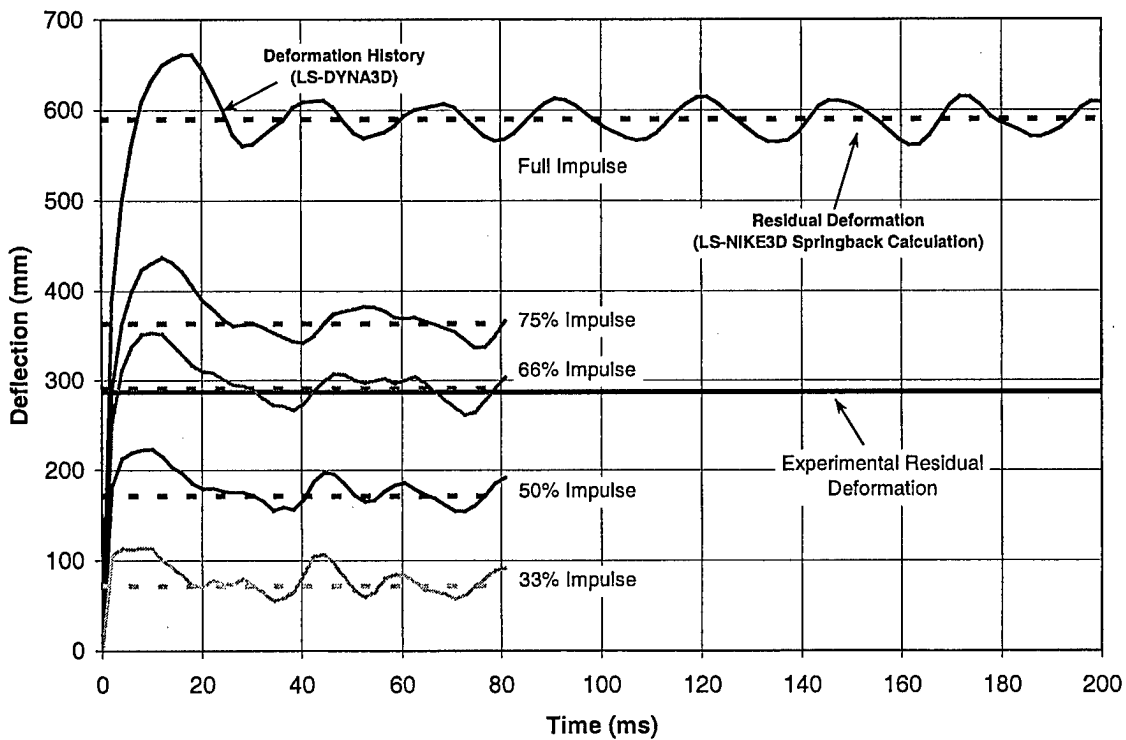


FIGURE 8 - Predicted peak floor deformation history as a function of impulse scaling factor for a 7.5-kg (16.5-lb) C-4 charge

The residual hull deformation resulting from the scaled impulse is shown in Fig. 9.

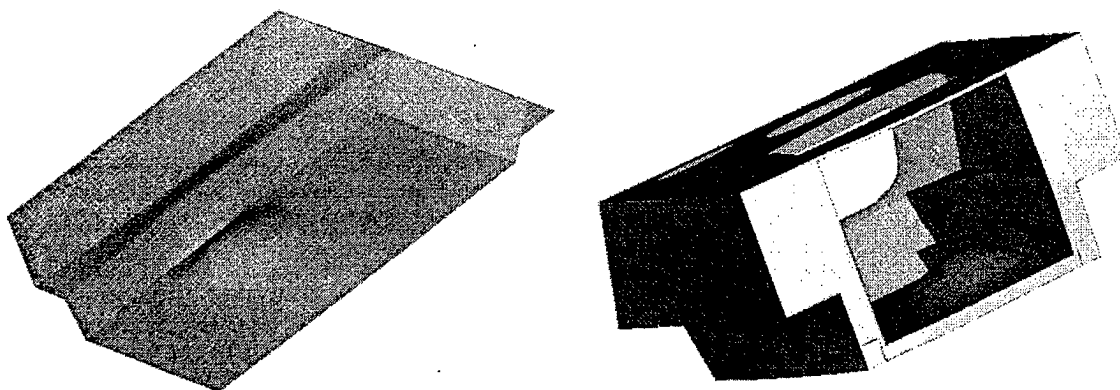


FIGURE 9 - Predicted floor deformation resulting from the 66% scaled impulse of a buried 7.5-kg (16.5-lb) C-4 charge

It is difficult to visually compare the predicted and measured overall deformation profiles of the floor. However, if we take slices along the length and across the width of the vehicle, through the point of maximum deflection, it is possible to get an idea of the accuracy of the numerical prediction. The comparisons, shown below in Fig. 10, demonstrate that the numerical model not only captures the peak residual deflection but it also accurately predicts the floor deflection profile.

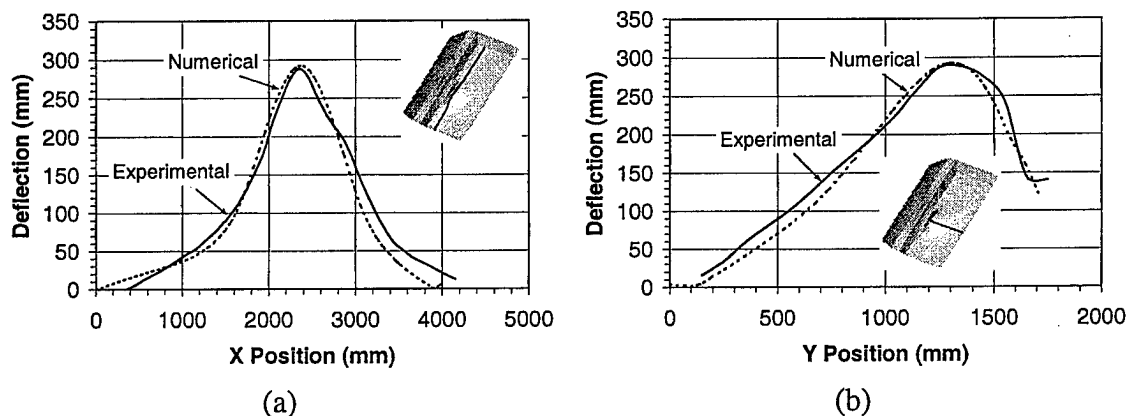


FIGURE 10 - Comparison of measured (solid line) and predicted (dashed line) residual floor deflection profiles through the point of maximum deflection (a) along the length of the vehicle and (b) across the width of the vehicle. The numerical results are for a simulation using a 66% scaled impulse of a buried 7.5-kg (16.5-lb) C-4 charge. The experimental results were obtained from St-Jean (Ref. 4).

Figure 11 shows the peak (transient) and residual (permanent) deformation as a function of the scaled impulse. Also shown is the residual displacement that is attributed to elastic deformation. This elastic deformation was estimated by subtracting the residual displacement from the peak dynamic deformation.

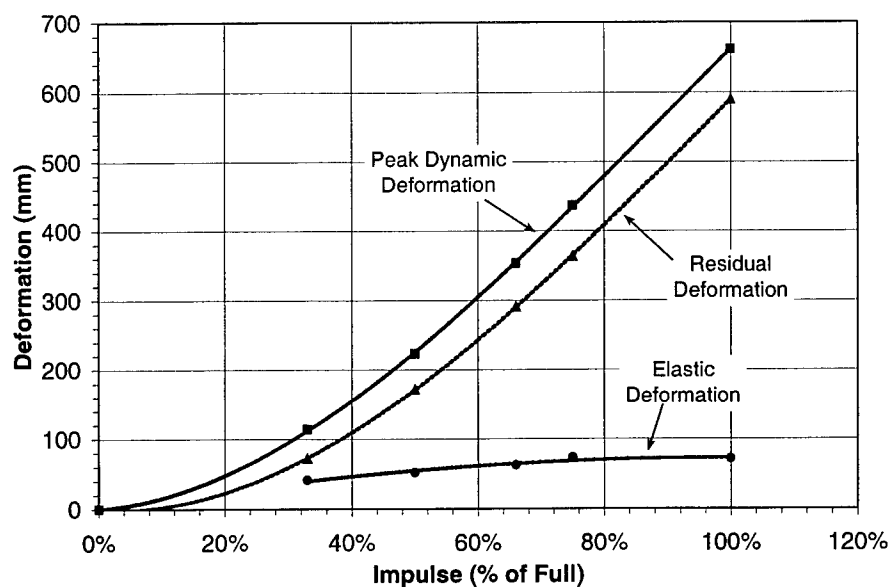


FIGURE 11 - Peak, residual, and elastic (estimated) deformation of impulse scaling factor for a 7.5-kg (16.5-lb) C-4 charge

It is interesting to note that the elastic deformation increases only gradually with increasing impulse. This would seem to indicate that the effect of the blast is predicted to be very localised. The overall size of the indentation does not increase much with increasing impulse. Instead the energy is absorbed through greater and greater plastic deformation of the floor directly over the detonation. The amount of deformation will be limited by the ultimate strength of the aluminum or by failure of a weld or joint.

Fig. 12 shows the plastic strain in the hull predicted for the scaled impulse. The maximum predicted plastic strain of 18.3% occurs where the floor panel meets the box beam that runs the length of the floor. Although specific material strength data for the Al 5086 H32 aluminum used in the M113A2s tested was not available, the maximum elongation for similar materials is approximately 9%. The butt weld that joins the large

floor panel to the box beams on either side further adds to the potential vulnerability of this part of the floor. Hull fracture would therefore be predicted at this location.

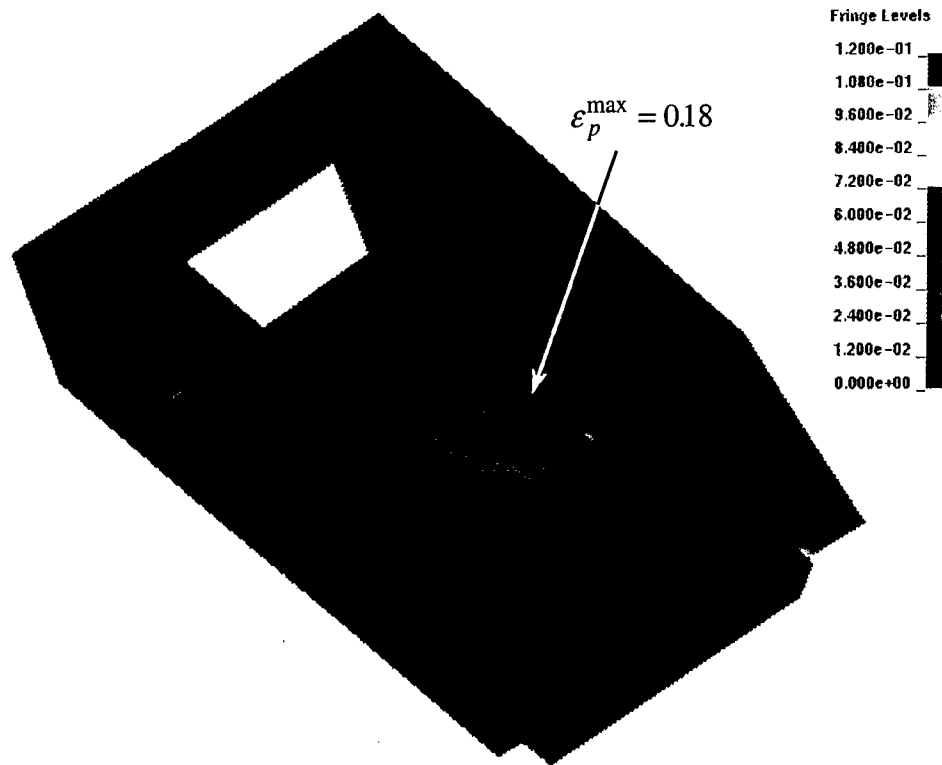


FIGURE 12 – Predicted plastic strain at $t = 200.0$ ms for a 7.5-kg (16.5-lb) charge of C-4 (note the steel armour plate has been removed for clarity)

Referring back to Fig. 1, a post-test photograph of the floor of a M113A2, one can clearly see a hull fracture along the inner edge of the box beam directly over the location of the blast, exactly the location that would be predicted by the model.

3.4 Implications of Scaling the Impulse

The relationship between the effective mine mass and the impulse predicted by Eqn. 1 is plotted in Fig. 13.

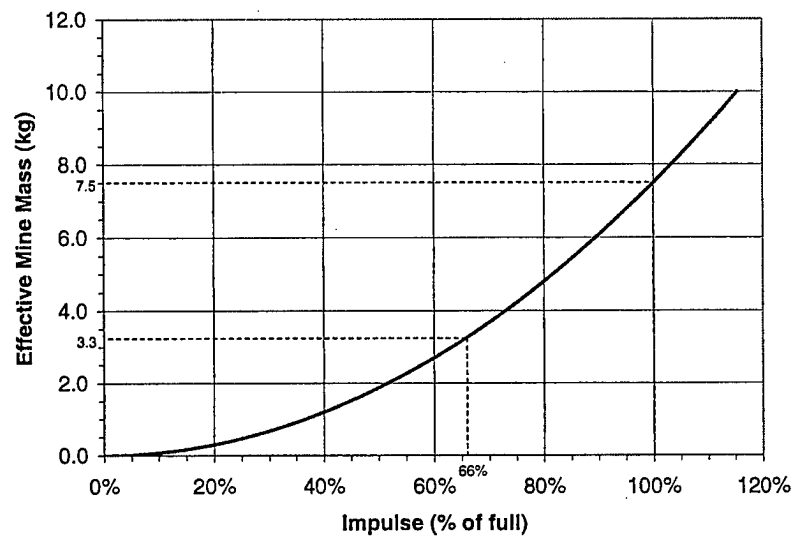


FIGURE 13 - Effective charge size as a function of impulse scaling factor

The scaled impulse, which gave good agreement with experimental measurements of peak floor deflection, is equivalent to the impulse for a 3.3-kg charge of C-4. As the energy release of the explosive is directly proportional to the mine mass, this represents a reduction in the effective energy release of the blast of 56% (energy release is proportional to the charge size, Eqn. 3). Although this may seem significant, this amount of energy can easily be attributed to absorption in the soil. Bergeron *et al.* (Ref. 9), for example, indicate that ground shock intensity can vary by two orders of magnitude depending on the soil and the moisture content. It is therefore possible that scaling of the energy release of the charge (i.e. scaling the impulse) was required because of energy absorption mechanisms that are not accounted for in the empirical equations through its dependence on the soil density alone.

4.0 CONCLUSION

In this study, an empirical model for predicting the impulse imparted to a flat plate by the detonation of a buried blast mine has been used to derive the boundary conditions for an explicit finite element analysis of the floor deflection of a modified M113A3 with upgraded floor protection. The results of this study indicate that the initial velocity distribution which is predicted by the empirical equations can result in an accurate assessment of the deformation of the hull. However, the peak residual deformation predicted is much higher than that observed experimentally. This over-prediction is attributed to the effect of the soil on detonation of a blast mine. Moisture content, temperature, and soil type are known to influence the energy absorbing qualities of the soil and hence the energy and momentum of the detonation products impinging on the target. The empirical model accounts for all of these variables through a single parameter, soil density.

In order to be able to use the empirical impulse loading model as a fully predictive tool, a better understanding of the relationship between the predicted impulse and the soil conditions is required. While no mechanism is available in the empirical equations to directly account for variations in the soil conditions, it may be possible to define a scaling factor based on soil type, soil moisture content, temperature etc. In this analysis, a factor of 66% was found to give good agreement with the experimental data. Further study is required to verify that this 33% reduction in impulse (a 56% reduction in the effective energy release of the charge) is in fact related to difference in the soil conditions at DREV and at the test site used during the calibration of the empirical model.

The other effect which was assumed to be insignificant but which will also have a measurable effect on the predicted deformation is strain rate hardening of the steel and aluminum. More accurate characterisations of the two materials will be incorporated into future simulations. The effects of weld strength is also a topic of interest as rupture of the hull may lead to venting of the hot combustion gases and debris into the crew

compartment. The model predictions showed plastic strains in excess of the approximate maximum elongation of the Al 5086 H32 aluminum.

Development of the M113 model will continue with the addition of the engine. The hatches, wheels, and other structures with significant mass and inertia will also be added to the shell model of the vehicle. The goal is to be able to perform a full analysis of the deformation and rigid body motion of the vehicle. The final model will be used to assess more accurate loading models (e.g. more detailed empirical loading models, combined CFD/CSD analyses, or Arbitrary Lagrangian/Eulerian or ALE analyses), as they become available.

5.0 ACKNOWLEDGEMENTS

The authors wish to acknowledge Dr. Dennis Nandlall, Dr. Grant McIntosh, and Mr. Benoît St-Jean for their comments and suggestions with regard to the numerical model and the simulations performed, as well as for the review of this document.

6.0 REFERENCES

1. Westine, P.S., Morris, B.L., Cox, P.A., and Polch, E.Z., "Development of Computer Program for Floor Plate Response from Land Mine Explosions", Technical Report No. 13045, US Army Tank-Automotive Command, Warren, MI, January, 1985, UNCLASSIFIED.
2. Morris, B.L., "Analysis of Improved Crew Survivability in Light Vehicles Subjected to Mine Blast, Volume 1 - Technical Report", SwRI Project No. 06-5095, Technical Report to U.S. Army Belvoir Research, Development and Engineering Centre, Virginia, December, 1993, UNCLASSIFIED.
3. Tremblay, J., "Impulse on Blast Deflectors from a Landmine Explosion", DREV-TM-9814, September, 1998, UNCLASSIFIED.
4. St-Jean, B., "Effects of Anti-Tank Mines on Prototype MTVL Fuel Cells", DREV Technical Memorandum under preparation.
5. Hallquist, J.O., "LS-DYNA Theoretical Manual", Livermore Software Technology Corporation, Livermore, CA, 1998.
6. FEMAP 6.0, Enterprise Software Products Inc., Exton, PA, 1999.
7. Hallquist, J.O., "LS-NIKE3D Theoretical Manual", Livermore Software Technology Corporation, Livermore, CA, 1998.
8. Maker, B., "User's Guide to Coupled Springback Calculations using LS-DYNA3D and LS-NIKE3D", Livermore Software Technology Corporation, Livermore, CA, March, 1996.
9. Bergeron, D., Walker, R., and Coffey, C., "Detonation of 100-Gram Anti-Personnel Mine Surrogate Charges in Sand - A Test Case for Computer Code validation", DRES-SR-668, Defence Research Establishment Suffield, Alberta, October, 1998, UNCLASSIFIED.

UNCLASSIFIED

INTERNAL DISTRIBUTION

DREV TM - 2000 - 007

1 – Director General
1 – Deputy Director General
1 – Chief Scientist
1 – Head, Weapon Effects Section
6 – Document Library
1 – Dr. K. Williams (author)
1 – Dr. D. Nandlall
1 – Mr. J. Tremblay
1 – Mr. M. Szymczak
1 – Dr. G. McIntosh
1 – Dr. C. Fortier
1 – Mr. D. Bourget
1 – R. Durocher, Capt
1 – Mr. B. St-Jean
1 – Mr. G. Pageau

UNCLASSIFIED

EXTERNAL DISTRIBUTION

DREV TM - 2000 - 007

- 1 - DRDCIM
- 1 - DRDCIM (unbound copy)
- 1 - DRDB
- 1 - DSTL 2
- 1 - DSTL 5
- 3 - DLR 3
- 2 - DLR 6
- 2 - DLR 7
- 1 - DOR (J&L)
- 1 - DRES
Attn: Dr. Chris Weickert
- 1 - National Library of Canada
- 1 - CISTI
- 1 - DTIC
- 1 - Mr. Kevin Poon (co-author)
6280 Garrison Court
Richmond, BC V7C 5H6
- 1 - DSTO
Aeronautical and Marine Research Laboratory
PO Box 1500
Salisbury 5108
SA, Australia
Attn: Dr. John Wang
- 1 - DERA Chertsey
Chobham Lane
Chertsey
Surry KT16 0EE
United Kingdom
Attn: Mark Saunders

UNCLASSIFIED

- 1 – Livermore Software Technology Corporation
7374 Las Positas Road
Livermore, California
USA 94550
Attn: Dr. J.O. Halquist
- 1 – Department of Civil Engineering
University of British Columbia
Vancouver, BC V6T 1Z4
Attn: Dr. Reza Vaziri
- 1 – Department of Mechanical Engineering
University of Waterloo
Waterloo, ON N2L 3G1
Attn: Dr. Michael Worswick

UNCLASSIFIED
SECURITY CLASSIFICATION OF FORM
(Highest classification of Title, Abstract, Keywords)

DOCUMENT CONTROL DATA														
1. ORIGINATOR (name and address) DREV	2. SECURITY CLASSIFICATION (Including special warning terms if applicable) UNCLASSIFIED													
3. TITLE (Its classification should be indicated by the appropriate abbreviation (S, C, R or U)) A NUMERICAL ANALYSIS OF THE EFFECT OF SURROGATE ANTI-TANK MINE BLASTS ON THE M113														
4. AUTHORS (Last name, first name, middle initial. If military, show rank, e.g. Doe, Maj. John E.) Williams, Kevin and Poon, Kevin														
5. DATE OF PUBLICATION (month and year) MARCH, 2000	6a. NO. OF PAGES 26	6b. NO. OF REFERENCES 9												
7. DESCRIPTIVE NOTES (the category of the document, e.g. technical report, technical note or memorandum. Give the inclusive dates when a specific reporting period is covered.) DREV TECHNICAL MEMORANDUM														
8. SPONSORING ACTIVITY (name and address) DLR 3														
9a. PROJECT OR GRANT NO. (Please specify whether project or grant) Work Unit 2fg16	9b. CONTRACT NO.													
10a. ORIGINATOR'S DOCUMENT NUMBER TM 2000-007	10b. OTHER DOCUMENT NOS N/A													
11. DOCUMENT AVAILABILITY (any limitations on further dissemination of the document, other than those imposed by security classification) <table style="width: 100%; border: none;"><tr><td style="width: 20px;"><input checked="" type="checkbox"/></td><td>Unlimited distribution</td></tr><tr><td><input type="checkbox"/></td><td>Contractors in approved countries (specify)</td></tr><tr><td><input type="checkbox"/></td><td>Canadian contractors (with need-to-know)</td></tr><tr><td><input type="checkbox"/></td><td>Government (with need-to-know)</td></tr><tr><td><input type="checkbox"/></td><td>Defense departments</td></tr><tr><td><input type="checkbox"/></td><td>Other (please specify)</td></tr></table>			<input checked="" type="checkbox"/>	Unlimited distribution	<input type="checkbox"/>	Contractors in approved countries (specify)	<input type="checkbox"/>	Canadian contractors (with need-to-know)	<input type="checkbox"/>	Government (with need-to-know)	<input type="checkbox"/>	Defense departments	<input type="checkbox"/>	Other (please specify)
<input checked="" type="checkbox"/>	Unlimited distribution													
<input type="checkbox"/>	Contractors in approved countries (specify)													
<input type="checkbox"/>	Canadian contractors (with need-to-know)													
<input type="checkbox"/>	Government (with need-to-know)													
<input type="checkbox"/>	Defense departments													
<input type="checkbox"/>	Other (please specify)													
12. DOCUMENT ANNOUNCEMENT (any limitation to the bibliographic announcement of this document. This will normally correspond to the Document Availability (11). However, where further distribution (beyond the audience specified in 11) is possible, a wider announcement audience may be selected.) Same as 11														

UNCLASSIFIED
SECURITY CLASSIFICATION OF FORM
(Highest classification of Title, Abstract, Keywords)

UNCLASSIFIED
SECURITY CLASSIFICATION OF FORM
(Highest classification of Title, Abstract, Keywords)

13. ABSTRACT (a brief and factual summary of the document. It may also appear elsewhere in the body of the document itself. It is highly desirable that the abstract of classified documents be unclassified. Each paragraph of the abstract shall begin with an indication of the security classification of the information in the paragraph (unless the document itself is unclassified) represented as (S), (C), (R), or (U). It is not necessary to include here abstracts in both official languages unless the text is bilingual).

This memorandum summarises numerical analyses which were performed to investigate the use of a simple empirical impulse loading model as a tool for modelling blast mine loading on a structure. The empirical model was used to generate the initial velocity boundary condition for an explicit dynamic finite element analysis of the floor deformation of a simulated M113 MTVL (upgraded floor protection) subject to the detonation of a buried 7.5-kg C-4 mine surrogate. Results showed an over-prediction of the peak residual floor deflection. Reducing the impulse by 33% gave excellent agreement with experimental results. The need to scale the impulse is attributed to energy absorption in the soil through mechanisms that are not accounted for in the empirical model. Moisture content and soil type, for example, are known to significantly affect the apparent strength of blast mines.

14. KEYWORDS, DESCRIPTORS or IDENTIFIERS (technically meaningful terms or short phrases that characterize a document and could be helpful in cataloguing the document. They should be selected so that no security classification is required. Identifiers, such as equipment model designation, trade name, military project code name, geographic location may also be included. If possible keywords should be selected from a published thesaurus, e.g. Thesaurus of Engineering and Scientific Terms (TEST) and that thesaurus-identified. If it is not possible to select indexing terms which are Unclassified, the classification of each should be indicated as with the title.)

Finite Element
LS-DYNA3D
Mine Blast
Protection
Numerical Simulation
Hydrocode Simulation
M113
MTVL
Blast Impulse

UNCLASSIFIED
SECURITY CLASSIFICATION OF FORM
(Highest classification of Title, Abstract, Keywords)